ABC Triblock Copolymers/Epoxy−Diamine Blends. 1. Keys To Achieve Nanostructured Thermosets

S. Ritzenthaler,[†,‡] F. Court,*,[§] L. David,[‖] E. Girard-Reydet,[†] L. Leibler,[⊥] and J. P. Pascault*,[†]

Laboratoire des Matériaux Macromoléculaires UMR CNRS 5627, Institut National des Sciences Appliquées, Bât. Jules Verne, 20 Avenue Albert Einstein, 69621 Villeurbanne Cedex, France; Centre d'Etude de Recherche et Développement ATOFINA, 27470 Serquigny, France; GEMPPM, UMR−CNRS 5510, Institut National des Sciences Appliquées, Bât. Jules Verne, 20 Avenue Albert Einstein, 69621 Villeurbanne Cedex, France; and Laboratoire Matière Molle et Chimie, UMR ESPCI−CNRS-ATOFINA, 10 rue Vauquelin, 75231 Paris Cedex 05, France

ABSTRACT: Epoxy thermoset blended with polystyrene-*block*-polybutadiene-*block*-poly(methyl methacrylate) triblock copolymers have been investigated before and after the epoxy−amine reaction, coupling different techniques: dynamic mechanical thermal analysis (DMTA), transmission electron microscopy (TEM) and small-angle X-ray scattering (SAXS). Before reaction, the three blocks self-organize on a nanometer scale, in PS spheres surrounded by PB nodules while the PMMA blocks are solubilized with the epoxy precursors, forming a swollen corona. Using MCDEA as hardener, the domain sizes were found not to be affected throughout the network formation. The final structure is composed of undiluted PS and PB blocks forming a "spheres on spheres" morphology, most of the PMMA chain remaining embedded in the epoxy network. A partial deswelling of the PMMA brush does occur during the epoxy−amine reaction, resulting in a pure PMMA phase. This phase, evidenced by DMTA, is most likely located at the vicinity of the interface with the PB microdomains. On the other hand, using DDS as hardener induces the phase separation of the PMMA blocks in the early stages of reaction, leading to flocculated, micrometer size elongated nanostructures and opalescent materials. Transparent nanostructurated thermosets were obtained when the following requirement was met: that the PMMA homopolymer remained soluble within the growing thermoset polymer during the whole reaction. The effects of "impurities" on the triblock behavior have also been studied and compared to the effects of "impurities" on a diblock behavior.

I. Introduction

Block copolymers have attracted considerable attention due to their wide variety of nanostructures. These microphase-separated structures result from the competition between chain connectivity and block immiscibility. The morphologies of pure diblock copolymers can almost be predicted thanks to a good knowledge of factors dictating geometry.[1−5] In AB diblock copolymers, the morphology is primarily governed by the composition of the block copolymers, expressed by the volume fraction of each component, and by the interaction parameter between blocks. Concerning ABC triblock copolymers consisting of three different components A, B and C, phase separation results in a greater variety of morphologies since the formation of microphase-separated assemblies is influenced by two independent composition parameters: the volume fraction of components A and B, and the relative immiscibility expressed by the interfacial tension γ_{ij}, or by the interaction parameter χ_{ij}, between the directly connected A/B, B/C and the "nonlinked" blocks A/C.[1,2] In the literature

devoted to triblock copolymers, the most important theoretical[8] and experimental studies have been carried out on polystyrene-*block*-polybutadiene-*block*-poly(methyl methacrylate), SBM.[9−12] For such triblock copolymers, the morphology is influenced by the repulsive forces between the polybutadiene (PB) mid block and both polystyrene (PS) and poly(methyl methacrylate) (PMMA) end blocks. More recently the morphological behavior of a polystyrene-*block*-polybutadiene-*block*-poly(ethylene oxide) triblock copolymer has been studied.[13]

Block copolymers are known to have the ability to form micelles in a nonreactive selective solvent. For an AB diblock copolymer in a selective solvent which is good for A but poor for B, the block copolymer molecules tends to associate into B core/A shell spherical micelles.[14] In blend applications, the solvent is usually an homopolymer (H) with the same chemical nature than one of the block (A) of the copolymer.[15−18] In these systems, a certain amount of homopolymer can be dissolved in the copolymer, depending on the molar mass of the homopolymer (M_H) regarding to that of the corresponding block (M_A) of the copolymer. If $M_H < M_A$, homopolymer can be substantially solubilized in the corresponding domain of the copolymer. Above the solubility threshold, a phase separation occurs between the swollen copolymer and the pure homopolymer.

Earlier work[19] on block copolymers dissolved in reactive solvents like styrene has been revalorized recently using thermoset (TS) precursors like epoxy[20−23] and phenolic[24] systems. In classical thermoplastic-modified TS, the thermoplastic and the TS precursor are initially

* To whom correspondence should be addressed. (F.C.) Telephone: 02.32.46.67.38. E-mail: Francois-Court@atofina.com. (J.P.P.) Telephone: 04.72.43.82.25. Fax: 04.72.43.85.27, E-mail: pascault@insa-lyon.fr.
 † Laboratoire des Matériaux Macromoléculaires UMR CNRS 5627, Institut National des Sciences Appliquées.
 ‡ Present address: Dow Deutschland Inc., D-77836 Rheinmuster, Germany.
 § Centre d'Etude de Recherche et Développement ATOFINA.
 ‖ GEMPPM, UMR-CNRS 5510, Institut National des Sciences Appliquées.
 ⊥ UMR ESPCI-CNRS-ATOFINA.

miscible. During the curing process of the TS precursor, the molar mass increase involves a decrease in the conformational entropy of mixing, and the phase separation between the thermoplastic and the step-growing thermoset network occurs, generally well before gelation.[25] In contrast to classical linear homopolymers, macroscopic phase separation can be avoided with block copolymers. It was demonstrated that amphiphilic diblock copolymers, with one block miscible with the TS, are not only dispersible in a reactive system but also able to order themselves on the nanometer scale in both the unreacted and reacted states.[20-24] Important applications are expected from this behavior.

Bates et al.[20,21] blended a poly(ethylene oxide)-*block*-poly(ethylene-*alt*-propylene) (PEO-*b*-PEP) symmetrical diblock copolymer of low molar mass with an epoxy system. The selected epoxy prepolymer, a classical diglycidyl ether of bisphenol A (DGEBA), is initially a selective solvent for the PEO chains. DGEBA was reacted with methylene dianiline as hardener (MDA). The evolution of the morphology during reaction was recorded by small-angle X-ray scattering (SAXS). No macrophase separation could be observed between the diblock and the epoxy during the whole reaction process. As PEO is expulsed from the epoxy network only at a local scale, the fully cured material presents a well-defined ordered nanostructure. This phenomenon is explained by a synergy between the curing reaction, local phase separation and energy barriers to nucleation of block copolymers rich domains. Block copolymers incorporating an epoxy-reactive functionality in one block, poly(epoxyisoprene)-*block*-polybutadiene or poly-(methyl acrylate-*co*-glycidyl methacrylate)-*block*-polyisoprene have also been studied as modifiers for epoxy networks,[22] and the conclusions were similar. In the same way, nanostructured phenolic networks have been obtained with the use of poly(2-vinylpyridine)-*b*-poly-isoprene.[24]

Mülhaupt et al.[26,27] incorporated low molar mass polycaprolactone-*block*-poly(dimethylsiloxane), (PCL)$_2$-*b*-PDMS-*b*-(PCL)$_2$, branched triblock copolymers in an epoxy matrix. The aim was to improve mechanical properties of epoxy network with the immiscible elastomeric PDMS blocks compatibilised by the PCL segments, initially miscible in epoxy precursors. Even if the structure obtained before reaction is not detailed, elastomeric particles of 20 nm in diameter, uniformly dispersed in the epoxy matrix, are generated at the end of the curing process. Concerning the mechanical properties, the addition of small amount of triblock copolymer leads to an increase of the toughness by a factor of more than two, for copolymer contents of 5 wt % or more, without reduction of the strength at break and Young's modulus by comparison with the neat epoxy system.

The aim of this work was to generate nanostructured thermoset materials using ABC triblock copolymers. For that purpose, a polystyrene-*block*-polybutadiene-*block*-poly(methyl methacrylate), SBM copolymer has been selected, knowing that (i) the homopolybutadiene used, PB, is immiscible with the epoxy precursor, leading to an initial macrophase separation between PB rubber and epoxy monomers,[28] (ii) the homopolystyrene used, PS, is initially partially miscible with the epoxy precursors (a homogeneous solution is obtained at temperature higher than 90 °C, whereas decreasing temperature

involves phase separation between homopolystyrene and the epoxy monomers), and (iii) the homopoly(methyl methacrylate) used, PMMA, was previously shown to be completely miscible with epoxy precursors.[29] This work differs from the previous studies[20-24] on block copolymers/thermoset blends by the fact that the selected copolymer is a high molar mass ABC triblock and it contains a PMMA block. That triblock copolymer was also synthesized anionically at pilot scale by Atofina[30] and due to the synthesis process, some SB diblock copolymer is inherently present in the initial product. Even if SBM purification can be easily achieved, the effect of these "impurities" on the generated structures was investigated. Finally, our attempt was also to highlight the advantages of such SBM triblocks compared to similarly synthesized BM diblocks containing PB impurities.

This part was restricted to the study of blends based on one, purified or as received triblock and two epoxy systems. The various factors affecting the morphologies and properties will be studied in a second part.[31]

II. Experimental Part

II.1. Techniques. Size Exclusion Chromatography. A Waters device, equipped with a 6000A pump, an U6K-type injector, and a double detection instrument (UV at $\lambda = 254$ nm and a differential refractometer R401) was employed. The eluent was tetrahydrofuran (THF) at a flow rate of 1 mL·min^{-1} at 20 °C.

Small-Angle X-ray Scattering. Small-angle X-ray scattering experiments have been carried out on a setup including a rotating anode, X-ray generator with copper target ($\lambda = 1.54$ Å). Point collimation is achieved with Franck mirrors and detection with a line position sensitive proportional counter. The scattered intensity was collected at room temperature, and studied as usual as a function of the scattering vector q ($q = 4\pi/\lambda \sin \theta$, 2θ being the scattering angle) in the range $0.005-0.1$ Å^{-1}.

Results have been analyzed using the model developed by Beaucage for correlated domains or particles.[32-33] Accordingly, the scattered intensity is given by

$$\overline{I(q)} = A F(q)^2 \, S(q)$$

with $S(q)$ the factor that accounts for weak correlations of the domains and $AF(q)^2$ describing the scattered intensity of isolated domains and

$$AF(q)^2 = I_0 \exp(-R_g^2 q^2/3) + C\left[\frac{[\text{erf}(qR_g/\sqrt{6})]^3}{q}\right]^P \quad (1)$$

with $P = 4$. I_0 is an exponential prefactor and R_g is the gyration radius of the particle.

This equation is designed to describe the evolution of the scattered intensity in the entire scattering vector q range. In the low-q range of the scattering diagrams, only the Guinier term, $I_0 \exp(-R_g^2 q^2/3)$ of the above equation is dominant, and if the fit is restricted to the scattering range where $qR_g < 1$, then the generalized Porod term, namely $I_{\text{Por}}(q) = C[[\text{erf}(qR_g/\sqrt{6})]^3/q]^p$ can be neglected for the sake of programming simplicity.

Moreover, $S(q)$ is a semiempirical function describing correlation of colloidal particles or domains in terms of a radius of correlation, ζ, and a packing factor k:

$$S(q) = \frac{1}{1 + k\Phi} \quad (2)$$

k describes the degree of correlation between particles and reaches its maximum of about 6 for closed packed crystal
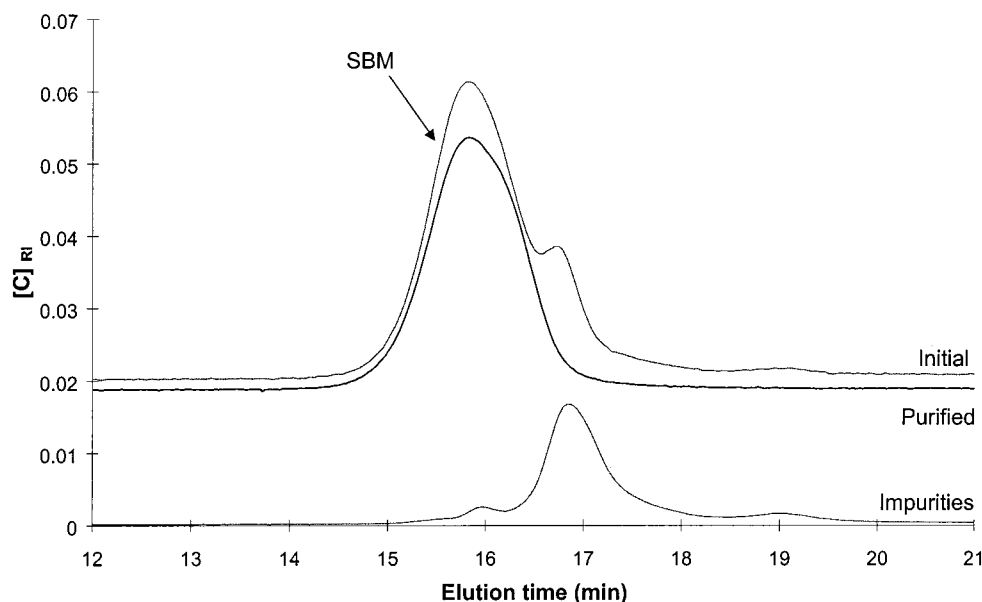
Figure 1. SEC chromatogram of SBM triblock copolymer: initial (SBM−SB), purified (SBM), and its "impurities" (SB).

structure. In our case, we observe values for k lower than 4, consistent with weak correlations. Besides, Φ is given by

$$\Phi = 3\frac{\sin{(q\zeta)} - q\zeta\cos(q\zeta)}{(q\zeta)^3} \qquad (3)$$

Transmission Electron Microscopy. Transmission electron microscopy analyses were carried out on a Philips CM120 microscope operating at 80 kV. Ultrathin sections were obtained using two different techniques:

1. The sample is cut using an ultramicrotome equipped with a diamond knife, to obtain 60 nm thick ultrathin sections. Then, the sections are stained on nickel grids with osmium tetraoxide vapors during 2 h.

2. For samples with rigidity not high enough to prepare high quality ultrathin sections at room temperature, a pyramid-shaped piece is cut and treated with a 4% aqueous solution of osmium tetraoxide during 1 week. Ultrathin sections are then microtomed on the flat top of the pieces.

Considering the applied staining conditions, PB appears black, PS gray, and PMMA whiter than the epoxy network.[34]

Dynamic Mechanical Analysis. Dynamic mechanical analysis (DMA) was carried out on cured blends with a Rheometrics solid analyzer (RSAII) in order to obtain tensile dynamic mechanical spectra (storage modulus E', loss modulus E'', and loss factor tan δ) between 50 and 250 °C at a frequency of 1 Hz. The samples used were parallelepipedic bars ($1 \times 2.5 \times 34$ mm³).

II.2. Materials. SBM Triblock Copolymer. The triblock used was an asymmetric polystyrene-*block*-polybutadiene-*block*-poly(methyl methacrylate), SBM copolymer synthesized anionically at pilot scale by Atofina.[30,35] The PMMA block is highly syndiotactic (>70%), and the PB structure is more than 85% 1,4. Because of the synthesis process, some SB diblock copolymer is present in the initial product. The purification can be achieved by precipitating the initial SBM in cyclohexane at 80 °C three times successively. Cyclohexane is then removed during 20 h under vacuum and pure SBM, SB "impurities" are isolated. Figure 1 presents the size exclusion chromatograms obtained for the initial copolymer, the purified copolymer, and the "impurities".

The composition was determined coupling ^{1}H nuclear magnetic resonance (^{1}H NMR) and size exclusion chromatography (SEC) methods. During the synthesis, an aliquot of PS is extracted before the addition of butadiene monomers. The molar mass of the PS block is then obtained by SEC in tetrahydrofuran (THF), using PS standards. Moreover, compositions are determined using ^{1}H NMR. Thus, the molar mass

Table 1. Characteristics of the Copolymer Used

Purified triblock copolymer						
Composition			Weight percentage			Nomenclature
S	B	MMA	S	B	MMA	
						$S^{27}_{22}B_9M_{69}$
27 000	11 000	84 000	122 000 g/mol	22	9	69

As received triblock copolymer		
Purity (weight percentage)		Nomenclature
SBM	SB	
79	21	$S^{27}_{22}B_9M_{69}$−SB21

of each block can be calculated using the molar mass of PS block and the mass fraction of PS in the copolymer.

The SB "impurities" concentration can also be determined coupling ^{1}H NMR results for the initial copolymer and the calculated purified copolymer composition.

In this paper, the nomenclature used is similar to the one proposed by Stadler et al.:[11] $S^x_t B_u M_v$ with t, u, and v corresponding to the mass percent of blocks determined by ^{1}H NMR and x to the PS block number-average molar mass in kg mol⁻¹, determined by SEC. Concerning the initial block copolymer containing "impurities", the nomenclature will be $S^x_t B_u M_w$−SBo with o the weight percentage of diblock SB.

The characteristics of the block copolymer used in this part I are given in Table 1. S and B blocks have the same molar mass in triblock and "impurities".

Thermoset Precursors. The epoxy monomer used is a diglycidyl ether of bisphenol A (DGEBA) with an average number of hydroxyl groups per two epoxy groups $\bar{n} = 0.15$ (LY556 from Vantico). The hardener used are two aromatic diamines, the 4,4′-methylenebis [3-chloro 2,6-diethylaniline] (MCDEA) from Lonza and the 4,4′-diamino diphenyl sulfone (DDS) from Fluka. The characteristics and structures of monomers are listed in Table 2. The epoxy monomer and the diamine are used in stoichiometric proportions.[29]

II.3. Samples Preparation. Block Copolymer Films. The neat copolymer is dissolved in THF and cast into flat-bottomed Petri dishes by slowly evaporating the solvent at 20 °C over a period of 1 week. The samples are further dried under vacuum for 12 h to ensure complete removal of the solvent.

Blend Preparation. Concerning blends with thermoset precursors, the concentration of block copolymers was fixed to 50 wt % in this part I. They were prepared either by solvent
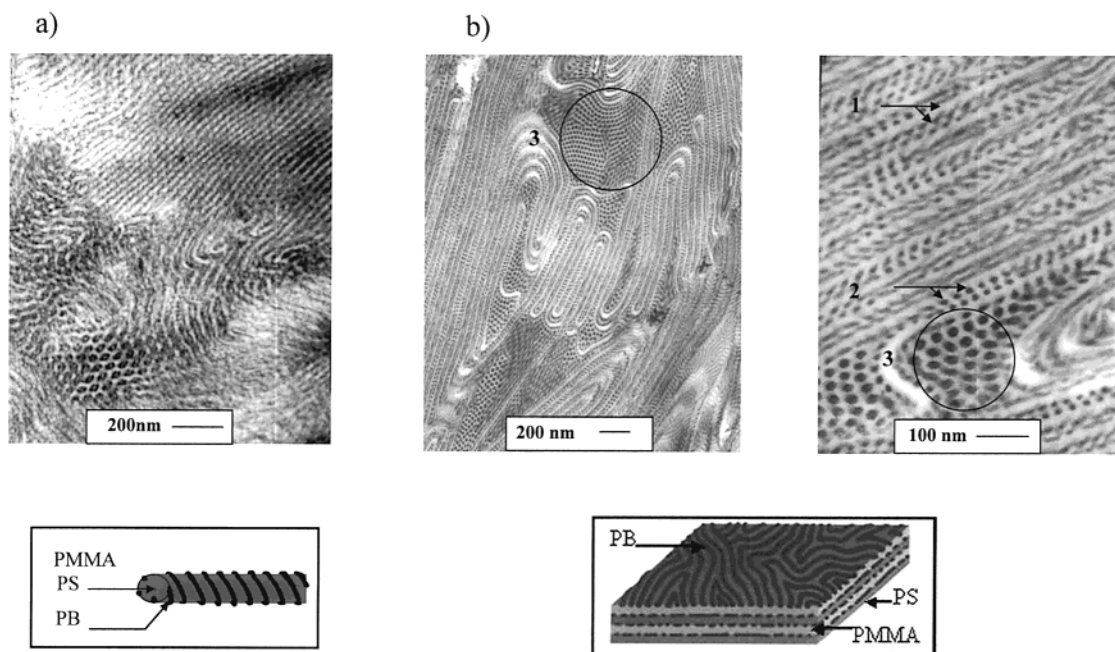
Figure 2. Transmission electron micrograph (O_SO_4 staining) of the triblock copolymer and the schematic representation of the structures: (a) purified $S_{22}^{27}B_9M_{69}$; (b) as received $S_{22}^{27}B_9M_{69}$–SB21. Films are obtained by solvent casting.

Table 2. Characteristics of Thermoset Monomers Used

| Name	Chemical Structure	Molar Mass (g/mol)	Supplier
Diglycidyl ether of bisphenol A (DGEBA)		382.6 $\bar{n}$=0.15	Ciba Geigy
4,4'-methylenebis-[3-chloro 2,6 diethylaniline] (MCDEA)		380	Lonza
4,4'-diaminodiphenyl sulfone (DDS)		248	Fluka

casting, as described above, or by mechanical mixing. In that last case, a homogeneous premix containing 10 wt % copolymer was prepared in a glass reactor at 135 °C. The other 40 wt % copolymer were then mixed to the premix in a twin-screw kneader for 1 h at 135 °C. The diamine was added over 5 min. For curing, the blend was pressed in a mold at 135 °C during 24 h and postreacted for 4 h at 190 or 220 °C for MCDEA- or DDS-based systems, respectively.

III. Results and Discussion

III.1. Morphologies of Neat SBM Triblock Copolymers.

Before studying blends, it was useful to know the morphologies of the block copolymers in bulk. Figure 2a displays typical electron micrograph of purified $S_{22}^{27}B_9M_{69}$ sample obtained by solvent casting in THF. A helical morphology of PB helices turning around a PS cylinder in a matrix of the main component PMMA can be observed. A schematic description of the structure is given below the micrograph.

The formation of morphologies in the SBM system is governed by the relatively weak immiscibility of the PS

and PMMA blocks compared to the strong immiscibility of the PB mid block, respectively, $\chi_{SM} \ll \chi_{SB} < \chi_{MB}$,[7] and by the volume fraction of components. In our case, considering the respective molar mass of each block, the PMMA block has the highest volume fraction. The same structure than the one in Figure 2a) has already been obtained by Krappe et al.[10] for a high molar mass triblock copolymer with a similar composition, $S_{25}B_{12}M_{63}^{218}$ (in this nomenclature, 218 is the molar mass of the copolymer in kg mol^{-1}). They observed that this helical morphology could only be obtained with high molar mass block copolymer, lower molar mass inducing a core–shell morphology. The dynamic mechanical spectrum obtained with our purified triblock copolymer, $S_{22}^{27}B_9M_{69}$ film is presented in Figure 3. As expected three different α relaxations are observed: the α relaxation of the PB blocks around −90 °C, a relaxation at 98 °C corresponding to the α relaxation of the PS blocks, and a third one at 132 °C, corresponding to the α relaxation of the syndiotactic PMMA blocks.
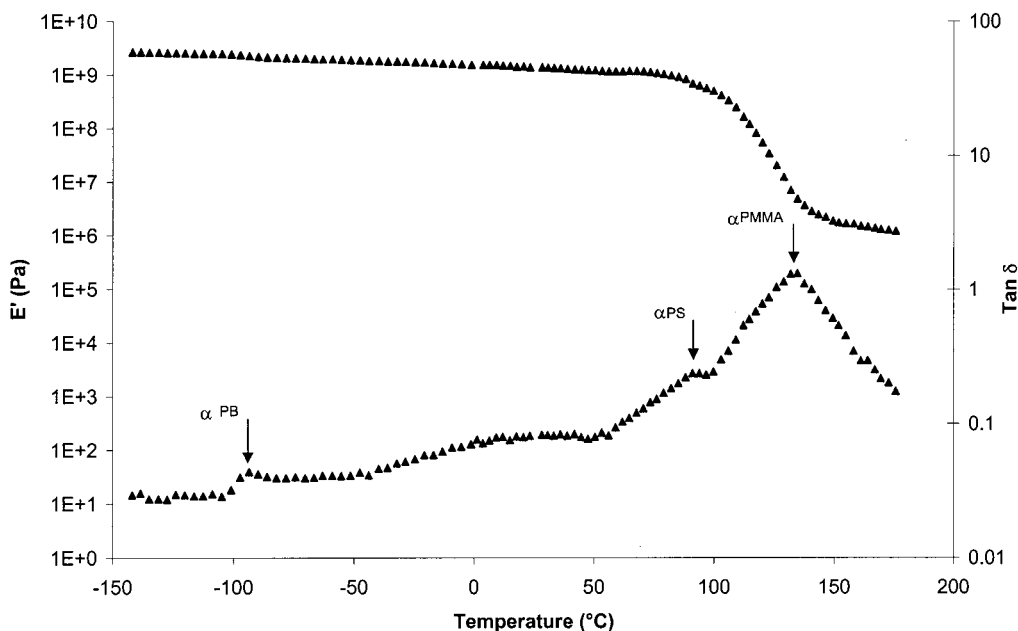
Figure 3. Dynamic mechanical spectra obtained at 1 Hz for the purified block copolymer $S_{22}^{27}B_9M_{69}$.

Concerning the as-received $S_{22}^{27}B_9M_{69}$–SB21 block copolymer (Figure 2b), a lamellar structure of PS and PMMA blocks (arrow 1) is observed with dark domains at the PMMA/PS phase boundary depicting the presence of PB cylinders (arrow 2). Because the ultrathin sections may be cut perpendicular, diagonal or parallel to the cylinder direction, the PB cross sections appear as spherical, ellipsoidal or cylindrical areas. Below micrograph Figure 2b is given a schematic representation of the structure taking into account that PB cylinders do not exhibit perfectly rectilinear organization. Moreover, some macroseparated domains corresponding to isolated SB diblocks (Figure 2b, arrow 3) and composed of PB cylinders hexagonally packed in a PS matrix are also observed.

It has been shown that the mixture of ABC triblock and AB diblock copolymer could result in different morphologies.[12,36,37] First, the two kinds of block copolymers can macrophase separate, forming individual domains with morphologies identical to those obtained for the corresponding pure block copolymers. Oppositely, the diblock can incorporate into the triblock copolymer structure at a molecular level, that is to say that the A blocks are mixed inside each A domain. For large amounts of diblock, the change in volume fraction of A and B will induce a modification of the interface curvature and thus on the morphology. Birshtein et al.[36,37] have shown that the interfacial tension between components, γ, plays a crucial role in the morphological behavior of blends of block copolymers. It was confirmed experimentally by Abetz and Goldacker[12] who observed miscible ABC + AB mixtures when $\gamma_{AB} > \gamma_{BC}$, while macrophase separation occurred in the blends where $\gamma_{AB} < \gamma_{BC}$.

The block length is the other important parameter. In our case, the presence of macrophase-separated SB domains (arrow 3, Figure 2b) may then be linked to the fact that $\gamma_{SM} < \gamma_{SB} < \gamma_{BM}$. Nevertheless, the change from an helicoidal (nonpurified SBM) to a lamellar (purified SBM) structure concurrently attests from the incorporation of part of SB diblock into the SBM structure, that leads to an effective increase of the volume fraction of both PS and PB relative to PMMA.

That partial incorporation of SB diblock is certainly favored by the low molar mass PB blocks and the high PMMA volume fraction.

III.2, Nanostructured Epoxy Networks from Purified Triblock Copolymers. Choice of the TS Precursors. Our choice of polyepoxide precursors was governed by the solubility in the epoxy monomers of the homopolymers corresponding to each block in the epoxy monomers.

The homoPB is known to be totally immiscible with the epoxy prepolymer DGEBA, leading to a macrophase separation between practically pure PB and DGEBA.[28] The homoPS is partially miscible with DGEBA. The cloud point curve exhibits an upper critical solution temperature, UCST, and the miscibility window depends on the molar mass of the blend components. It also depends on the epoxy hardener used.[29,38] The addition of MCDEA at stoichiometry leads to a shift of the UCST curve toward lower temperatures, and the addition of DDS leads to the opposite trend.

During reaction, DGEBA–MCDEA is a better solvent than DGEBA–DDS for homoPS, resulting in a higher extent of reaction at phase separation, x_{CP}. Typically for a homoPS with a number-average molar mass, $M_n = 80$ kg mol^{-1}, and at a curing temperature $T_i = 135$ °C, $x_{CP} \sim 0.20$ for a DGEBA–MCDEA system, and $x_{CP} \sim 0.01$ for a DGEBA–DDS one.

On the other hand, homoPMMA was shown to be initially miscible and to remain miscible with DGEBA–MCDEA reacting system during the whole reaction process, whatever the concentration and the curing temperature. With DGEBA–DDS, homoPMMA is initially miscible but macrophase separate during reaction. At curing temperature $T_i = 135$ °C, $x_{CP} \sim 0.30$.[29]

Both DGEBA–MCDEA and DGEBA–DDS systems were then selected and compared to investigate the effect of PMMA block miscibility on the final structures.

Purified Triblock in DGEBA–MCDEA. The morphology of DGEBA–MCDEA/50 wt % $S_{22}^{27}B_9M_{69}$ blend is presented in Figure 4a before reaction, at two different magnifications. The blend is initially transparent and remains transparent after reaction (Figure 4b). The ordered nanostructures before and after reaction are
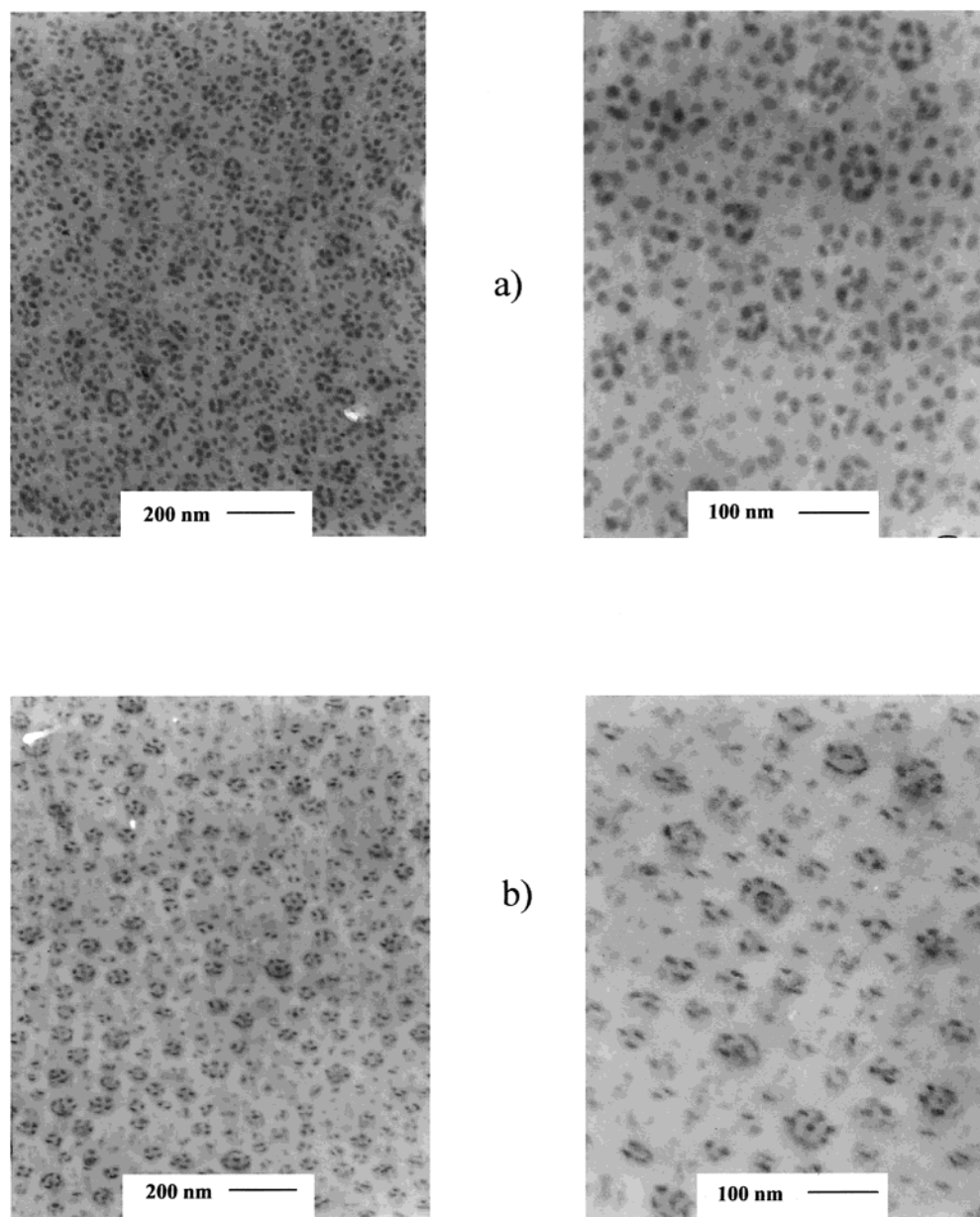
Figure 4. Transmission electron micrographs obtained for the DGEBA−MCDEA/50 wt % $S_{22}^{27}B_9M_{69}$ blend (a) before and (b) after reaction.

quite similar: (i) the epoxy-rich phase forms the matrix despite the high block copolymer concentration; (ii) the dark nodules, with sizes in the range 10 nm, correspond to the microphase-separated PB blocks, and the bright domains to the microphase-separated PS blocks.

To confirm the existence of two different kinds of domains, the same samples have been analyzed by SAXS. Before reaction the same scattering spectra has been obtained at room temperature and at 135 °C. The blends before and after reaction, exhibit two distinct Guinier regimes on the SAXS profiles, indicating a spatial organization of two different domains with characteristic sizes. The radii of the diffusing species involved have been determined using the model developed by Beaucage et al.[32,33] for weakly correlated domains dispersed in a medium. The weak correlation hypothesis is noted by the absence of any significant correlation peak on the spectra (not shown here).

The results are listed in Table 3. The largest domains, 30 nm, are attributed to the PS spheres whereas the

Table 3. Radii Obtained by SAXS Measurements of the PS and PB Domains for Blends with 50 wt % $S_{22}^{27}B_9M_{69}$ before and after Reaction

|		nodules radii, nm	
reaction	temp, °C	PS	PB
before	20	30	12
	135	30	12
after	135	29	11

smallest radii, 12 nm, correspond to the PB particles. Before reaction, the temperature increase does not lead to any modification of the scattering domain sizes. This implies that the swelling of the PS blocks does not depend on the temperature. These results also strengthen the idea that the reaction has practically no effect on the nanostructure.

To further investigate the behavior of PMMA blocks, DMA has been carried out on the fully reacted sample between room temperature and 250 °C. In Figure 5 three different relaxations can be observed:
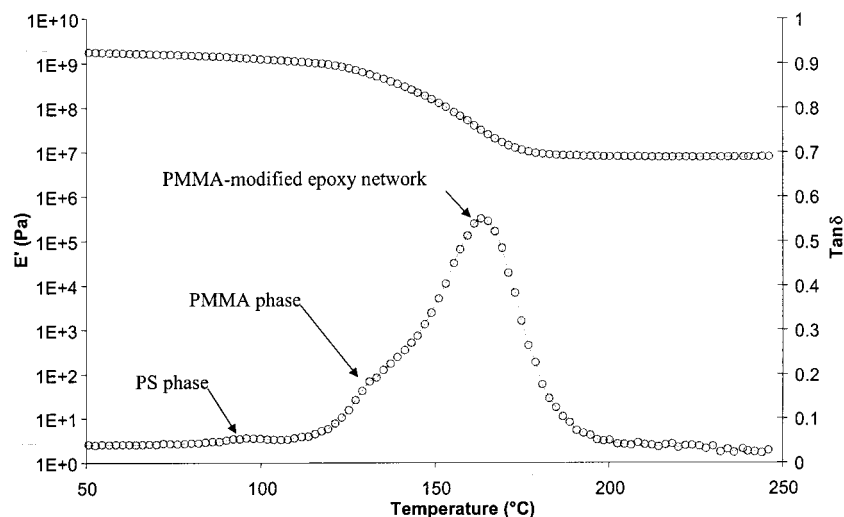
Figure 5. Dynamic mechanical spectra obtained at 1 Hz for the DGEBA−MCDEA/50 wt % $S_{22}^{27}B_9M_{69}$ blend after reaction.
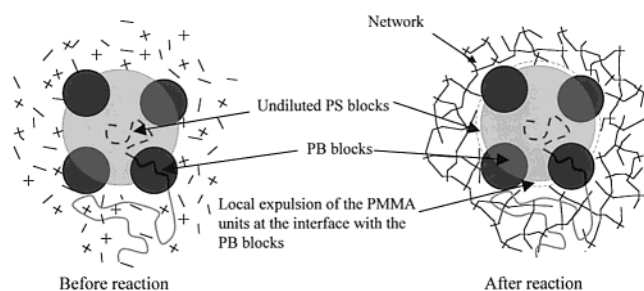
Figure 6. Schematic description of the evolution of the triblock organization in the DGEBA−MCDEA thermoset system before and after reaction.

(i) The first is the main relaxation at 163 °C, which is associated with the glass transition temperature of the epoxy-rich phase. The shift of this relaxation to lower temperature compared to the one of the neat DGEBA−MCDEA network (187 °C) indicates a plastification effect induced by the incorporation of PMMA blocks in the epoxy network. The same phenomena has already been observed for miscible DGEBA−MCDEA/homoPMMA blends.[29]

(ii) The second is a shoulder at 130 °C, corresponding to the relaxation of pure PMMA blocks (Figure 3), which denotes a partial microphase separation of some PMMA units from the epoxy-rich matrix.

(iii) The last is a low temperature relaxation peak at 97 °C, which confirms the presence of practically pure PS microdomains.

To summarize *all* of these TEM, SAXS and DMA results, a schematic representation of the triblock organization before and after reaction is given in Figure 6. Before reaction, the self-assembly process leads to the following morphology: the PB blocks aggregate into spherical domains at the interface between the epoxy-rich matrix and spheres formed by the PS blocks. Hence, the swelling of the PMMA blocks by epoxy components induces a morphological transition from PB helices around PS cylinders, the morphology of the neat triblock (Figure 2), to PB spheres on PS spheres. The structuration of PS and PB blocks is not affected by the reaction, meaning that the PS blocks are microphase separated from the epoxy system even before reaction. Moreover, it is clear from DMA results (Figure 5) that a partial deswelling of the PMMA brush occurs during the epoxy reaction. It can be reasonably assumed that

the initial morphology is preserved because this expulsion from the PMMA brush takes place at the latest stage of the reaction. The viscosity of the system is such that morphological rearrangements are hindered. This local expulsion of PMMA segments results from the reduction of entropy associated with the epoxy reaction: initially, the swelling of the PMMA brush is driven by the gain in conformational entropy brought to PMMA chains by the low molar mass epoxy precursors. While the epoxy network builds up, this gain disappears, the brush recovers its nonswollen state, "the brush dries out". It is therefore most likely, that the PMMA segments which are left pure after the expulsion of the epoxy network are the ones located at the vicinity of the interface with the PB microdomains as represented in Figure 6.

This result can be compared to the one obtained by Lipic et al.[21] concerning a nanostructured thermoset based on a similar epoxy system and a diblock copolymer, poly(ethylene oxide)-*block*-(polyethylene-*alt*-propylene), PEO-*b*-PEP. The PEO block is miscible with the epoxy precursors, though during its formation the network is expelled locally by the PEO brush. This expulsion is evidenced by the presence of a melting peak on the DSC scan of the fully reacted material, signature of a pure PEO phase.

It can be concluded that the immiscible mid block significantly reduces the solubility of both chemically linked PS and PMMA blocks by comparison to thermodynamic predictions from homopolymers. Nevertheless, in the present case of long PMMA blocks linked to short PB blocks, most of the PMMA blocks is not deswelled and remains as a "wet brush". Because of this efficient intermixing between PMMA blocks and the epoxy component, the resulting nanostructured material is expected to exhibit good adhesion and mechanical properties (see part 2[31]).

To demonstrate the necessity to have PMMA blocks, an experiment has been performed with a $S_{71}^{27}B_{29}$ diblock (the extracted diblock "impurity" of our as received triblock). Even if a good dispersion of this diblock in DGEBA−MCDEA monomers could initially be achieved macrophase separation rapidly occurs during curing leading to an opaque sample. The micrograph in Figure 7 shows that 2 μm diameter particles of SB diblocks have been pulled out during ultra microtoming due to the poor adhesion between the nodules of SB diblocks
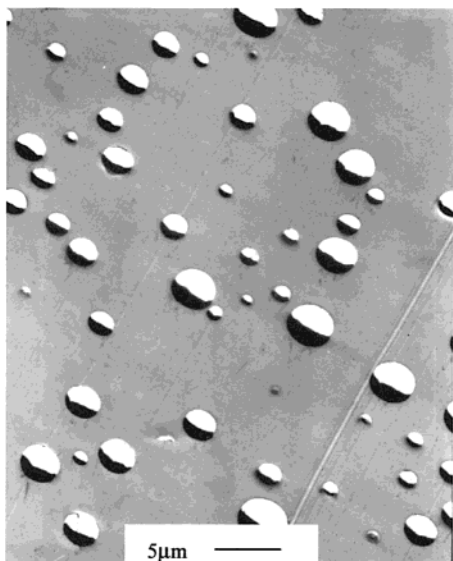
Figure 7. Transmission electron micrograph obtained for the DGEBA−MCDEA/10 wt % $S_{22}^{27}B_9$ blend after reaction.
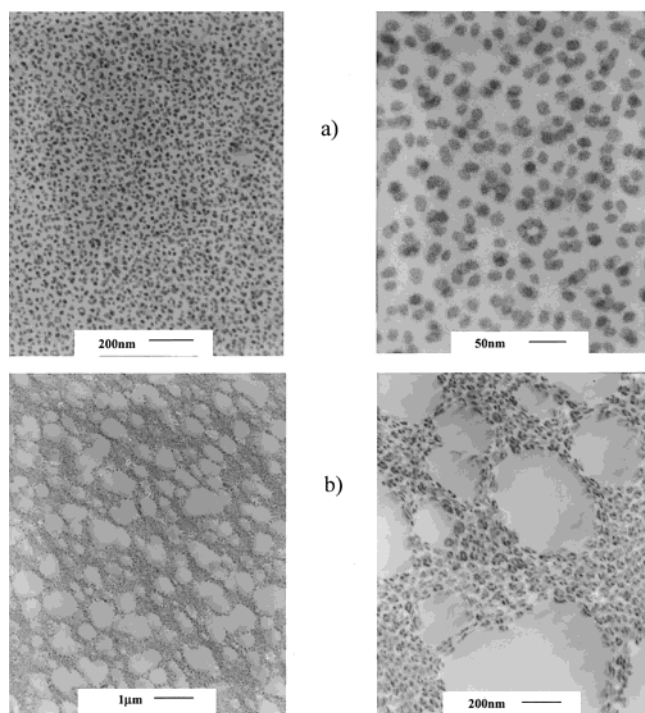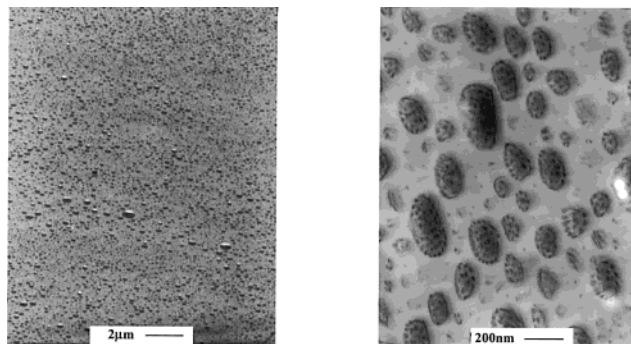

Figure 8. Transmission electron micrograph obtained for the DGEBA−DDS/50 wt % $S_{22}^{27}B_9M_{69}$ blend and (b) for the blend after reaction.

Figure 9. Transmission electron micrograph obtained for the DGEBA−MCDEA/50 wt % $S_{22}^{27}B_9M_{69}$ - SB21 blend after reaction at two scales.

and the epoxy matrix. A similar macrophase separation has recently been observed when a $S_{30}^{21}B_{70}$ diblock copolymer is blended with a diamine-cured poly(propylene oxide) type epoxy monomer.[39]

Purified Triblock in DGEBA−DDS. The morphology of DGEBA−DDS/50 wt % $S_{22}^{27}B_9M_{69}$ blend before reaction illustrated in Figure 8a is similar to that of the blend based on DGEBA−MCDEA (Figure 4a). It confirms that the main parameters dictating the structure are (i) the complete immiscibility of the PB blocks and (ii) the full solubility of the PMMA blocks.

Alternatively the behavior during reaction of the blend based on DGEBA−DDS is completely different and an opaque sample is finally generated indicating that reaction-induced macrophase separation has oc-

curred. Macrophase separation between the block copolymer and the DGEBA−DDS component is also clearly evidenced by TEM (Figure 8b). In this case during epoxy−amine reactions, the PMMA blocks phase separate at $x_{CP} \sim 0.30$ (well before gelation, $x_{gel} = 0.60$) and the triblock microparticles are consequently no further stabilized and flocculate. A bicontinuous structure at a macroscopic scale is then obtained, but it is worth noting that the initial organization of PB nodules surrounding PS microdomains at a nanometer scale is preserved. The triblock macrophase thus results from the aggregation (flocculation) process of these initial microparticles.

When core−shell preformed particles are blended with epoxy,[40] similar aggregation and flocculation effects have already been observed during reaction.

However, the comparison between the two epoxy systems clearly confirms that the obtention of nanostructured transparent networks requires the solubility of the corresponding homopolymer of one block with the growing thermoset polymer during the whole reaction process. Otherwise macrophase segregation takes place as in a classical thermoset/thermoplastic blend.[25]

III.3. Triblock SBM vs Diblock BM. To investigate the effect of SB "impurities" present in the industrial SBM, the morphology of the DGEBA−MCDEA thermoset in the presence of 50 wt % of the as-received $S_{22}^{27}B_9M_{69}$−SB21 triblock is shown after reaction in Figure 9 at two different magnifications.

Differently from the neat as received triblock, no macrophase-separated SB domains can be observed on the final microstructure. Then, when blended with epoxy, the as received triblock has the ability to fully incorporate SB "impurities" even if a solubility limit certainly exists. This obviously requires that PMMA blocks efficiently intermix with the epoxy component up to the end of the reaction. Compared to the blend with the purified triblock (Figure 4b), incorporation of SB combined with the decrease of the effective PMMA block fraction from 69 to 55% leads to an increase of the size of triblock segregated microdomains.

Finally to discuss the advantages of such SBM triblocks compared to similarly synthesized diblocks which can also favorably interact with epoxy, an asymmetric diblock copolymer (with the same PMMA concentration than SBM) has been synthesized, namely $B_{30}^8M_{70}$−B25, and purified, $B_{30}^8M_{70}$. Figure 10a shows the final structure after reaction of the DGEBA−MCDEA/10 wt % $B_{30}^8M_{70}$ blend. Well-ordered microparticles can be seen with radii $\sim$8 nm (SAXS measurements). Alternatively, when PB "impurities" are present in the BM diblock,
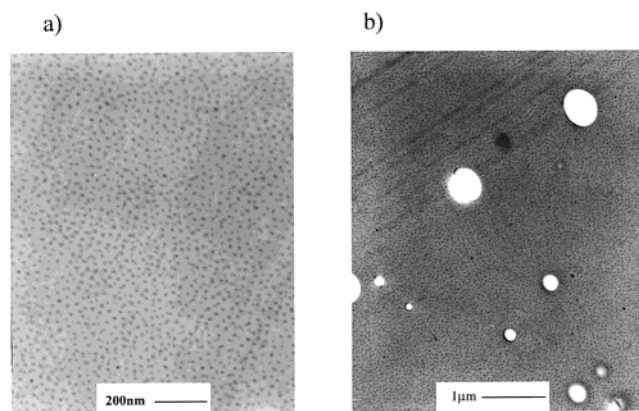
Figure 10. Transmission electron micrograph obtained for cured blends (a) DGEBA−MCDEA/10 wt % $B_{30}^8M_{70}$ and (b) DGEBA−MCDEA/10 wt % $B_{30}^8M_{70}$−B25.

DGEBA−MCDEA/10 wt % $B_{30}^8M_{70}$−B25 blend, the reacted sample is fully opaque with isolated macrophase-separated homoPB particles (Figure 10b). When blended with epoxy, the BM diblock is then unable to stabilize the "impurities".

Considering that industrial anionically prepared block copolymers with PMMA blocks, X−M, inherently contain precursor chains, X, one major advantage of SBM compared to BM is the ability to incorporate in the microstructure and thus stabilize its "impurities", i.e., the SB diblocks, a purification step being thus useless.

Conclusion

Transparent nanostructurated thermosets could be achieved by blending and reacting an epoxy system with SBM triblock, synthesized anionically at an industrial scale. The only requirement is the solubility of the corresponding PMMA homopolymer with the growing thermoset polymer during the whole reaction obtained when MCDEA is used as hardener. Otherwise, using DDS instead of MCDEA, macrophase separation takes place similarly to classical thermoset/thermoplastic blend. The strongly immiscible PB mid block significantly affects the solubility with epoxy, of the chemically linked PS blocks compared to its homopolymer. Indeed, whereas homoPS is initially miscible with epoxy monomers and phase separates during the reaction process, PS blocks were found to be microphase separated even before reaction. The structure of PS and PB blocks is therefore not affected by the reaction. Even if a local segregation of PMMA units at the vicinity of PB microdomains was revealed by viscoelastic measurements, the efficient intermixing of the main PMMA fraction with epoxy, up to the end of the reaction, ensures the structuration of the blend at a nanometer scale.

Because of the synthesis process, fractions of SB diblock copolymer are inherently present in the initial SBM. When blended with epoxy, the triblock used in this study was shown to have the ability to fully incorporate SB "impurities", through the absence of isolated macrophase-separated region and the only increase of the size of the triblock segregated microdomains. This constitutes their main advantage over similarly synthesized BM diblocks. The generation of nanostructurated thermosets from such industrial SBM does not require any purification step. The importance of stabilizing synthesis impurities on the material final properties, especially its toughness, will be discussed in a companion paper.[31]

References and Notes

(1) Helfand, E. *Macromolecules* **1975**, *8*, 552−556.
(2) Leibler, L. *Macromolecules* **1980**, *13*, 1602−1617.
(3) Matsen, M. W.; Bates, F. S. *Macromolecules* **1996**, *29*, 1091−1098.
(4) Quirk, R. P.; Kinning, D. J.; Fetters, L. J. *Comprehensive Polymer Science*; Aggarwal, S. L., Ed.; Pergamon Press: Oxford, England, 1989; Vol 7, pp 1−26.
(5) Riess, G. In *Thermoplastics elastomers, a comprehensive review*; Legge, N. R., Holden, G., Schroeder, H. E., Eds; Hanser: Munich, Germany, 1997.
(6) Bates, F. S.; Fredrickson, G. H. *Phys. Tod.* **1999**, February, 32−38.
(7) Stadler, R.; Auschra, C.; Beckmann, J.; Krappe, U.; Voigt-Martin, I.; Leibler, L. *Macromolecules* **1995**, *28*, 3080−3097.
(8) Zheng, W.; Wang, Z. G. *Macromolecules* **1995**, *28*, 7215−7223.
(9) Auschra, C.; Stadler, R. *Macromolecules* **1993**, *26*, 2171−2174.
(10) Krappe, U.; Stadler, R.; Voigt-Martin, I. *Macromolecules* **1995**, *28*, 4558−4561.
(11) Breiner, U.; Krappe, U.; Abetz, V.; Stadler, R. *Macromol. Chem. Phys.* **1997**, *198*, 1051−1083.
(12) Abetz, V.; Goldacker, T. *Macromol. Rapid Commun.* **2000**, *21*, 16−34.
(13) Bailey, T. S.; Pham, H. D.; Bates, F. S. *Macromolecules* **2001**, *34*, 6994−7008.
(14) Chu, B.; Liu, T.; Wu, C.; Zhou, Z. *Macromol. Symp.* **1997**, *118*, 221−227.
(15) Löwenhaupt, B.; Steurer, A.; Hellmann, G. P.; Gallot, Y. *Macromolecules* **1994**, *27*, 908−916.
(16) Lescanec, R. L.; Fetters, L. J.; Thomas, E. L. *Macromolecules* **1998**, *31*, 1680−1685.
(17) Jiang, M.; Cao, X.; Yu, T. *Polymer* **1986**, *27*, 1923−1927.
(18) Matsen, M. W. *Macromolecules* **1995**, *28*, 5765−5773.
(19) Finaz, G.; Skoulios, A.; Sadron, C. C. *R. Acad. Sci. Paris* **1967**, *253*, 565−569.
(20) Hillmyer, M. A.; Lipic, P. M.; Hadjuk, D. A.; Almdal, K.; Bates, F. S. *J. Am. Chem. Soc.* **1997**, *119*, 2749−2750.
(21) Lipic, P. M.; Bates, F. S.; Hillmyer, M. A. *J. Am. Chem. Soc.* **1998**, *120*, 8963−8970.
(22) Grubbs, R. B.; Dean, J. M.; Broz, M. E.; Bates, F. S. *Macromolecules* **2000**, *33*, 9522−9534.
(23) Mijovic, J.; Shen, M.; Sy, J. W.; Mondragon, I. *Macromolecules* **2000**, *33*, 5235−5244.
(24) Kosonen, H.; Ruokolainen, J.; Nyholm, P.; Ikkala, O. *Macromolecules* **2001**, *34*, 3046−3049.
(25) Pascault, J. P.; Williams, R. J. J. In *Polymer Blends*; Paul, D., Bucknall, C. B., Eds.; John Wiley: New York, 2000; Vol 1, pp 380−412.
(26) Buchholz, U.; Mülhaupt, R. *ACS Polym. Prepr.* **1992**, *33*, 205−206.
(27) Könczöl, L.; Döll, W.; Buchholz, U.; Mülhaupt, R. *J. Appl. Polym. Sci.* **1994**, *54*, 815−826.
(28) Chen, D.; Pascault, J. P.; Bertsch, R. J.; Drake, R. S.; Siebert, A. R. *J. Appl. Polym. Sci.* **1994**, *51*, 1959−1970.
(29) Ritzenthaler, S.; Girard-Reydet, E.; Pascault, J. P. *Polymer* **2000**, *41*, 6375−6386.
(30) Navarro, C.; Marcarian, X.; Vuillemin, B. *Macromol. Symp.* **1998**, *132*, 263−272.
(31) Ritzenthaler, S.; Court, F.; Girard-Reydet, E.; Leibler, L.; Pascault, J. P. Part 2. Submitted for publication.
(32) (a) Beaucage, G.; Schaefer, D. W. *J. Non-Cryst. Solids* **1994**, *172−174*, 797−805. (b) Beaucage, G.; Ulibarri, T. A.; Black, E. P.; Schaefer, D. W. In *Hybrid Organic−Inorganic Composites*; Mark, J. E., Lee, C. Y−C., Bianconi, P. A., Eds.; ACS Symposium Series 585; American Chemical Society: Washington, DC, 1995; pp 97−111.
(33) Guinier, A.; Fournet, G. *Small Angle Scattering of X-rays*; Wiley: New York, 1955; pp 42−65.

(34) Sawyer, L.; Grubb, D. T. *Polymer Microscopy*; Chapman and Hall; London, **1987**, 93−109.

(35) Jerôme, R.; Teyssie, P.; Vuillemin, B.; Zundel, T.; Zune, C. *J. Polym. Sci., Part A: Polym. Chem.* **1999**, *37*, 1−10.

(36) Birshtein, T.; Polotsky, A. A.; Amoskov, V. M. *Macromol. Symp.* **1999**, *146*, 215−222.

(37) Birshtein, T.; Zhulina, E. B.; Polotsky, A. A.; Abetz, V.; Stadler, R. *Macromol. Theory Simul.* **1999**, *8*, 151−160.

(38) Girard-Reydet, E.; Pascault, J. P.; Brown, H. *Macromolecules* **2001**, *34* n*o*. 15, 5349−5353.

(39) Guo, Q.; Figueiredo, P.; Thomann, R.; Gronski, W. *Polymer* **2001**, *42*, 10101−10110.

(40) Sue, H. J.; Garcia-Meitin, E. I.; Pickelman, D. M.; Yang, P. C. In *Toughened Plastics I− Science and Engineering*; Riew, C. K., Kinloch, A. J., Eds.; Advances in Chemistry Series 233; American Chemical Society: Washington, DC, 1993; pp 259−291.